Evaluation of the ejector two-stage compression refrigeration cycle with work performance from energy, conventional exergy and advanced exergy perspectives

Jing Xie (jxie@shou.edu.cn)
Shanghai Ocean University
Dazhang Yang
Shanghai Ocean University
Zhu Jie
Shanghai Ocean University
Yang Li
Shanghai Ocean University

Article

Keywords: carbon dioxide, trans-critical refrigeration, ejector, exergy destruction, energy analysis

Posted Date: March 15th, 2022

DOI: https://doi.org/10.21203/rs.3.rs-1420949/v1

Evaluation of the ejector two-stage compression refrigeration cycle with work performance from energy, conventional exergy and advanced exergy perspectives

Dazhang Yang [1,2,3,4,+], Zhu Jie [1,2,+], Yang Li [1,2,3,4], and Jing Xie [1,2,3,4,*]

[1] College of Food Science and Technology, Shanghai Ocean University, Shanghai 201306, China;
[2] Shanghai Professional Technology Service Platform on Cold Chain Equipment Performance and Energy Saving Evaluation, Shanghai 201306, China;
[3] Shanghai Engineering Research Center of Aquatic Product Processing & Preservation, Shanghai 201306, China;
[4] National Experimental Teaching Demonstration Center for Food Science and Engineering, Shanghai Ocean University, Shanghai 201306, China.;
[+] Dazhang Yang and Zhu Jie contributed equally to this study
[*] Correspondence: jxie@shou.edu.cn;

Abstract: Low temperature cold chain is the top priority of logistics development at this stage. CO_2 (carbon dioxide) refrigeration system is widely used. However, the low efficiency of CO_2 refrigeration system is the biggest obstacle to its development. In this research work, a novel trans-critical CO_2 refrigeration cycle with ejector for cryogenic storage is proposed. The energy and traditional exergy model of the system are established, and the advanced exergy model is established based on the traditional exergy model, and the actual performance of the system is analyzed. The results show that the exergy destruction of each component of the ejector is the largest in the system, and the optimization potential is the highest in both traditional and advanced exergy models. After studying the influence of main parameters in the system cycle on the system performance and performance, it is found that there is an optimum intermediate pressure and gas cooler pressure in the system to maximize the system performance and efficiency. According to the influence of the change of system parameters on the system, it is found that the outlet temperature of gas cooler has the greatest influence on the optimization of ejector.

Keywords: carbon dioxide; trans-critical refrigeration; ejector; exergy destruction; energy analysis

1. Introduction

In recent years, environmental problems caused by ozone depletion and greenhouse effect have become the focus of attention[1, 2]. Natural gas CO_2 has been discovered as a refrigerant in the refrigeration industry. Ozone depletion potential (ODP) is 0 and global warming potential (GWP) is 1, which are ideal refrigerants for sustainable development and have attracted more and more attention and research interest from all countries in the world[3]. The lower critical temperature of CO_2 is 31.1℃ and the critical pressure is up to 7.38MPa. Therefore, most CO_2 refrigeration cycles are conducted in the transcritical region [4-6]. These characteristics result in a high pressure ratio of the compressor in the refrigeration cycle, and an increase in pressure drop during throttling results in an increase in throttling losses, resulting in a lower efficiency of the CO_2 refrigeration system than other systems using freon refrigerants[7]. To improve the performance coefficient of R744 transcritical refrigeration/heat pump cycle, a new approach is proposed. Researchers have done a lot of research and summarized the following methods to improve system circulation performance: replacing throttle valve with expander or ejector, two-stage compression, mechanical supercooling, thermoelectric supercooling, swirl tube, parallel compression.

Introducing ejectors into the transcritical CO_2 refrigeration system instead of the throttle valve in the conventional cycle can improve system efficiency, improve the suction pressure of the compressor and regulate the flow relationship in the cycle[8]. Based on basic ejector circulating system, Zhang et al. [1] reviewed a large number of literature and summarized the improvement of CO_2 system performance by the use of ejector. The utility model has the advantages of simple structure and low cost and has broad application prospects in transcritical CO_2 refrigeration system. Song et al. [9] introduced and studied the model of two-phase flow ejector in an all-round way, and introduced the main problems of zero-one-dimensional model and three-dimensional model in the simulation of two-phase flow ejector, clarified the development status and existing problems of existing models, and considered that lack of clear understanding of complex thermodynamic mechanism of ejector was the biggest obstacle to its promotion. Santini et al. [10] used ejectors instead of expansion valves in the transcritical CO_2 vapor compression refrigeration cycle and considered that there was a strong correlation between COP and entrainment ratio (μ). Eskandari et al. [8] introduced a new type of transcritical CO_2 double injection refrigeration cycle. After the system was modeled, the cycle performance and exergy performance were compared with the conventional cycle by using EES (Engineering Equation Solver). It was found that the performance of the new cycle introduced after adjusting the different system parameters is 20-80% higher than that of the conventional cycle[11]. Nebot et al. [12] sought a high performance refrigeration system to optimize the performance of the system in actual operation. The experiments validated the existence of the optimum intermediate pressure and the optimum pressure of the gas cooler in the novel transcritical CO_2 refrigeration system. Liu et al. [13] analyzed a new transcritical CO_2 with double evaporator injection refrigeration cycle, analyzed the energy and exergy of the system, and compared it with the conventional system. It was found that the COP and exergy efficiency of the system is increased by 19.6% and 15.9% respectively under the set operating conditions.

Making use of the second law of thermodynamics, the analysis of refrigeration system is helpful to determine the most destructive position in the system, and to analyze the size of equipment exergy destruction in the system, to improve the system. Sun[14] and Liu[15] analyzed a large number of CO_2 transcritical refrigeration systems and found that the ejector most of exergy destruction in the refrigeration cycle. Dahmani et al. [16] studied the ejector refrigeration system, they found that more than half of the destruction in the ejector refrigeration system using R134a occurred in the ejector. Elbarghthi et al. [17] tested and analyzed the CO_2 transcritical ejector refrigeration system, evaluated the system parameters under different operating conditions, such as gas cooler pressure, outlet temperature of gas cooler, evaporation temperature and receiver. The experiment shows that with the increase of gas cooler pressure, the exergy destruction of the system gradually increases. It is also considered that in ejector-enhanced refrigeration systems, exergy analysis should be widely used to determine improvements made by ejector addition.

2. System description and assumptions

The schematic diagram and pressure enthalpy diagram of the transcritical CO_2 refrigeration system studied in this paper are shown in Figures 1(a) and (b). The refrigeration system replaces the conventional high-pressure side throttle valve with an ejector, which consists of a main nozzle, an injection chamber, a mixing chamber and a diffuser. In addition, it is composed of high-pressure compressor (HPC), gas cooler (GC), intercooler (ITC), internal heat exchanger (ITE), two-phase ejector (EJE), evaporator (EVA), low-pressure expansion valve (EV1), medium-pressure expansion valve (EV2) and low-pressure compressor (LPC).

The working cycle of the refrigerant in this cycle is as follows: the refrigerant high-pressure compressor in saturated vapor（state 1) coming from the intercooler, the compressed superheated vapor with high temperature and pressure (state 2) is cooled by the

gas cooler with constant pressure heat exchange (state 3) for heat exchange in the form of sensible heat. The refrigerant from the gas cooler exchanges heats twice by the internal heat exchanger for further supercooling (state 4). The supercooled refrigerant is sucked in by the main nozzle of the ejector. After depressurization by the nozzle, it is mixed with the medium-temperature medium-pressure refrigerant compressed by the low-pressure stage compressor introduced from the ejector chamber of the ejector. The two streams of fluid exchange momentum and energy in the mixing chamber of the ejector and are finally ejected in a two-phase flow state after pressurization by the diffuser (state 5). The refrigerant entering the intercooler exchanges heat with the refrigerant throttled by the medium-pressure throttle valve (state 11). The refrigerant in the mixed saturated vapor state in the intercooler is compressed by the high-pressure compressor. At the same time, the saturated refrigerant in the intercooler (state 6) is throttled by the low-pressure stage throttle valve (state 7) and enters the evaporator. After heat exchange through the evaporator (state 8), it enters the ITE for heat exchange again (state 9). Refrigerant enters the low-pressure compressor after heat exchange between the ITE and the high-pressure side fluid (state 10). One part of the compressed medium-temperature and medium-pressure refrigerant is mixed with the main body after being introduced by the ejector chamber and the other part enters the intercooler after being throttled by the medium-pressure throttle valve.

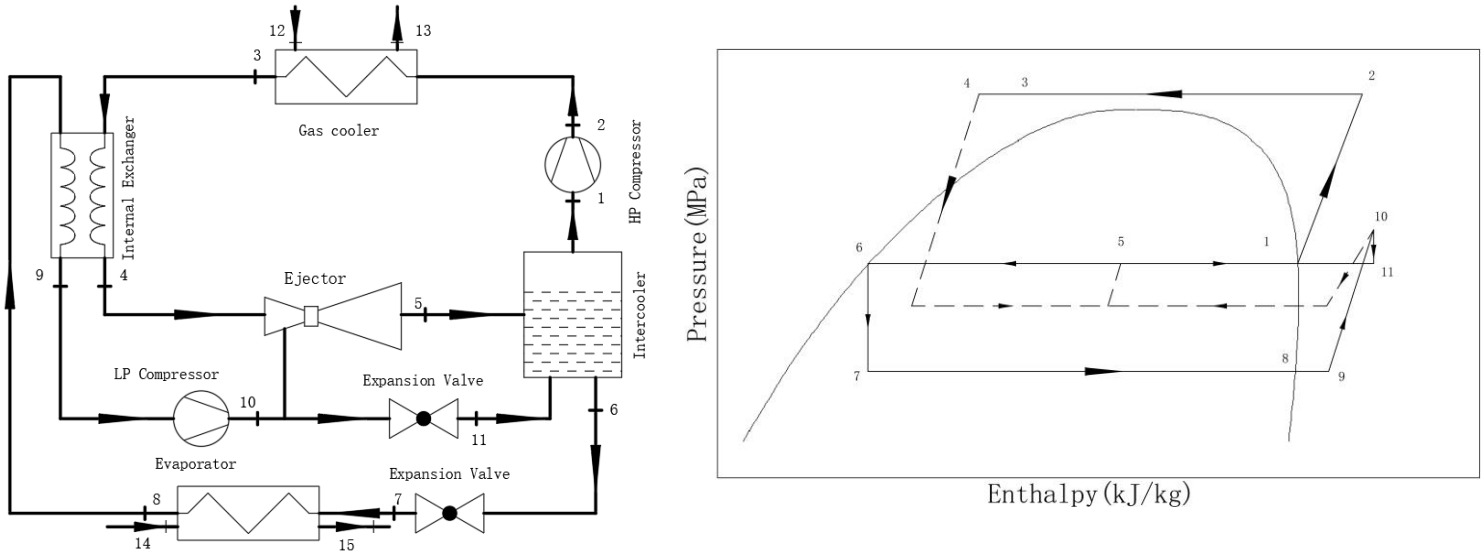

Figure 1. (a) Schematic diagram of transcritical CO_2 refrigeration system; **(b)** Pressure enthalpy diagram of transcritical CO_2 refrigeration system.

In order to simplify the simulation model, the following assumptions are made for the system:

(1) The compressor adopts adiabatic nonisentropic compression process, and the compression efficiency is obtained from the literature[18].

(2) The working efficiency of the main flow nozzle, suction chamber, mixing chamber and diffuser of the ejector is constant. The mixing section in the ejector carries out fluid mixing at constant pressure.

(3) The evaporator load at the low-pressure side of the system is calculated according to the previous calculation. Calculate the flow with 14.4kW. The system operates under the atmospheric conditions of $T_0 = 25$ ℃ and $P_0 = 101.325$kpa as the reference state.

(4) The system operates stably. Ignore the external heat loss caused by the medium pressure drop of connecting pipe, intercooler, gas cooler, evaporator and internal heat exchanger.

(5) The refrigerant flowing from the intercooler and evaporator is saturated.

(6) The temperatures of the liquid water at the inlet and outlet of the gas cooler remain fixed, T_{12}=26 ℃, T_{13}=61 ℃. Also, the air temperatures at the inlet and outlet of the evaporator are fixed at T_{14}=-25 ℃ and T_{15}=-30 ℃.

(7) The kinetic energy of the fluid passing through the inlet and outlet of the ejector is ignored.

3. Energy and conventional energy analysis

3.1. Energy model

Based on the above assumptions, the system model is modeled, and the basic equations can be obtained from the perspective of mass, momentum and energy conservation:

For HPC and LPC:

$$W_{LPC} = \dot{m}_l(h_{10} - h_9) = \dot{m}_l(h_{9,is} - h_9) / \eta_{LPC} \tag{0}$$

$$W_{HPC} = \dot{m}_h(h_2 - h_1) = \dot{m}_h(h_{1,is} - h_1) / \eta_{HPC} \tag{2}$$

$$\eta_{LPC} = 0.815 + 0.022(P_{10} / P_9) - 0.0041(P_{10} / P_9)^2 + 0.0001(P_{10} / P_9)^3 \tag{3}$$

$$\eta_{HPC} = 0.815 + 0.022(P_2 / P_1) - 0.0041(P_2 / P_1)^2 + 0.0001(P_2 / P_1)^3 \tag{4}$$

Among them, the compressor coefficient is obtained from the literature[18], which is specifically expressed as a function of the pressure relationship before and after the compressor.

For Cooling capacity of evaporator:

$$Q_e = \dot{m}_l(h_8 - h_7) \tag{5}$$

High and low pressure refrigerant flow ratio:

$$R_{mf} = \dot{m}_h / \dot{m}_l \tag{6}$$

For Intercooler:

$$(1+w)\cdot \dot{m}_h \cdot h_5 + (\dot{m}_h - w\cdot \dot{m}_l)\cdot h_{11} = \dot{m}_l \cdot h_1 + \dot{m}_h \cdot h_6 \tag{7}$$

For ejector:

$$w = \sqrt{\eta_n \eta_m \eta_d \frac{h_{n,in} - h_{n,out,is}}{h_{d,out,is} - h_{m,out}}} - 1 \tag{8}$$

$$h_4 + w\cdot h_{10} = (1+w)\cdot h_5 \tag{9}$$

The ejection ratio of the ejector is expressed by formula (8), and the detailed derivation process is shown in references[19].

For internal heat exchanger:

$$\dot{m}_l(h_9 - h_8) = \dot{m}_h(h_3 - h_4) \tag{10}$$

$$COP = Q_e / (W_{LPC} + W_{HPC}) \tag{11}$$

3.2. Conventional exergy analysis model

Exergy is the maximum useful work a system can delivered from a specified state to the state of its environment in theory. In order to evaluate the unavoidable exergy destruction of components in the system, further exergy analysis was carried out. The ratio exergy of refrigerants at each point of state can be defined as [20]:

$$\dot{E}_j = \dot{m} \cdot e = \dot{m} \cdot \left[\left(h_j - h_0 \right) - T_0 \left(s_j - s_0 \right) \right] \tag{12}$$

where subscript j represents the exergy state points 1-15 in Figure 1, and 0 represents the reference state point of the system (T_0 and P_0). The reference state is generally set to the ambient temperature, the specific enthalpy and specific Entropy of refrigerant at = 298.15K and = 101.325kPa.

The concept of exergy is defined by "fuel-products" and calculated by fuel exergy and product exergy as follows [21]:

$$\dot{E}_{F,k} = \dot{E}_{P,k} + \dot{E}_{D,k} \tag{0}$$

Exergy can be further divided into thermal exergy and mechanical exergy, expressed as [22]:

$$e = e_j^T + e_j^M = \left[\left(h_j - h_{P_j,T_0} \right) - T_0 \left(s_j - s_{P_j,T_0} \right) \right]_{P=const} + \left[\left(h_{P_j,T_0} - h_0 \right) - T_0 \left(s_{P_j,T_0} - s_0 \right) \right]_{T=const} \tag{0}$$

where the subscript k represents the k-th component in the system, which can be expressed as high-pressure compressor (HPC), gas cooler (GC), internal exchanger (ITE), ejector (EJE), expansion valve1 (EV1), evaporator (EVA), low-pressure compressor (LPC), expansion valve2 (EV2). The exergy of product ($\dot{E}_{P,k}$) represents the desired result of the component, The exergy of fuel ($\dot{E}_{F,k}$) contains all exergy of the component.

The exergy balance in the system is [23]:

$$\dot{E}_{F,tot} = \dot{E}_{P,tot} + \sum \dot{E}_{D,k} + \dot{E}_{L,tot} \tag{0}$$

where $\dot{E}_{F,tot}$ and $\dot{E}_{P,tot}$ are fuel exergy and product exergy in the system. $\dot{E}_{L,tot}$ is the exergy that can no longer be used in the system, which is only considered at the overall level of the system. and the specific calculation formula of exergy destruction of each component is listed in Table 1。

Table 1. The exergy destruction calculation equation in each component.

Components	$\dot{E}_{F,k}$ (kW)	$\dot{E}_{P,k}$ (kW)	$\dot{E}_{D,k}$ (kW)
Gas cooler	$E_{F,GC} = \dot{m}_h \cdot (e_2 - e_3)$	$E_{P,GC} = \dot{m}_{12} \cdot (e_{13} - e_{12})$	
Internal heat exchanger	$E_{F,ITE} = \dot{m}_h \cdot (e_3 - e_4)$	$E_{P,ITE} = \dot{m}_l \cdot (e_9 - e_8)$	
Ejector	$E_{F,EJE} = \dot{m}_h \cdot (e_4 - e_5)$	$E_{P,EJE} = w \cdot \dot{m}_h (e_{10} - e_5)$	
Intercooler	$E_{F,ITC} = \dot{m}_h \cdot (e_5 - e_1)$	$E_{P,ITC} = \dot{m}_l \cdot (e_6 - e_{11})$	
Expansion Valve 1	$E_{F,EV1} = \dot{m}_l \cdot (e_6^M - {}_7^M + e_6^T)$	$E_{P,EV1} = \dot{m}_l \cdot e_7^T$	$\dot{E}_{F,k} - \dot{E}_{P,k}$
Evaporator	$E_{F,EVA} = \dot{m}_l \cdot (e_7 - e_8)$	$E_{P,EVA} = \dot{m}_{14} \cdot (e_{15} - e_{14})$	
Low-pressure Compressor	$E_{F,LPC} = W_{LPC}$	$E_{P,LPC} = \dot{m}_l \cdot (e_{10} - e_9)$	
High-pressure Compressor	$E_{F,HPC} = W_{HPC}$	$E_{P,HPC} = \dot{m}_h \cdot (e_2 - e_1)$	
Expansion Valve 2	$E_{F,EV2} = (\dot{m}_l - w \cdot \dot{m}_h) \cdot (e_{10}^M - {}_{11}^M + e_{10}^T)$	$E_{P,EV1} = (\dot{m}_l - w \cdot \dot{m}_h) \cdot e_{11}^T$	

In the conventional exergy modelling, two parameters are defined to evaluate the component and system performance [24]:

$$\eta_k = \dot{E}_{P,k} / \dot{E}_{F,k} \tag{16}$$

$$\eta_{ex} = \dot{E}_{P,tot} / \dot{E}_{F,tot} \tag{0}$$

$$\delta_k = \dot{E}_{D,k} / \dot{E}_{D,tot} \tag{0}$$

$$\delta_{ex} = \dot{E}_{D,tot} / \dot{E}_{F,tot} \tag{19}$$

where η_k and η_{ex} are the exergy efficiency of the k-th component and overall system, and δ_k and δ_{ex} are the exergy destruction efficiency of the k-th component and overall system respectively.

3.3. Advance exergy analysis model

The size and location of irreversible loss in the system can be determined by conventional exergy analysis. However, there is no clear explanation on the deeper source of each component exergy destruction in the system [25, 26]. Advance exergy analysis overcomes the shortcomings of conventional exergy analysis, explains the relationship between various components in the system, evaluates the actual optimization potential of each component from another perspective, and has a deeper understanding of the improvement of system performance [27]. The exergy destruction of components is divided into avoidable/unavoidable and endogenous/exogenous parts [28].

Considering the economic and technical limitations of reducing exergy destruction, $\dot{E}_{D,k}$ can be divided into avoidable and unavoidable parts. Based on the relationship between various components in the system, $\dot{E}_{D,k}$ can be divided into endogenous/exogenous parts [24].

$$\dot{E}_{D,k} = \dot{E}^{UN}_{D,k} + \dot{E}^{AV}_{D,k} \tag{16}$$

$$\dot{E}_{D,k} = \dot{E}^{EN}_{D,k} + \dot{E}^{EX}_{D,k} \tag{17}$$

where $\dot{E}^{UN}_{D,k}$ and $\dot{E}^{AV}_{D,k}$ are unavoidable destruction due to technical limitations and avoidable exergy destruction, respectively. Therefore, more attention should be paid to the reduction of $\dot{E}^{AV}_{D,k}$ in the system. $\dot{E}^{EN}_{D,k}$ is related to the efficiency of the component itself and is endogenous. $\dot{E}^{EX}_{D,k}$ is caused by the irreversibility of other components of the system or the operation of the system and is external.

$$\dot{E}^{UN}_{D,k} = \dot{E}_{P,k} \left(\frac{\dot{E}_{D,k}}{\dot{E}_{P,k}} \right)^{UN} \tag{18}$$

where $\left(\frac{\dot{E}_{D,k}}{\dot{E}_{P,k}}\right)^{UN}$ is an inevitable factor in the refrigeration system, and this parameter is obtained under inevitable conditions [29].

The two segmentation methods are combined, that is, the relationship between components and the inevitable factors of the system can be considered [15].

$$\dot{E}_{D,k} = \dot{E}_{D,k}^{UN,EN} + \dot{E}_{D,k}^{UN,EX} + \dot{E}_{D,k}^{AV,EN} + \dot{E}_{D,K}^{AV,EX} \quad (19)$$

$$\dot{E}_{D,k}^{UN,EN} = \dot{E}_{P,k}^{EN} \left(\frac{\dot{E}_{D,k}}{\dot{E}_{P,k}} \right)^{UN} \quad (20)$$

$$\dot{E}_{D,k}^{UN,EX} = \dot{E}_{D,k}^{UN} - \dot{E}_{D,k}^{UN,EN} \quad (21)$$

$$\dot{E}_{D,k}^{AV,EN} = \dot{E}_{D,k}^{EN} - \dot{E}_{D,k}^{UN,EN} \quad (22)$$

$$\dot{E}_{D,k}^{AV,EX} = \dot{E}_{D,k}^{EX} - \dot{E}_{D,k}^{UN,EX} \quad (23)$$

where $\dot{E}_{D,k}^{UN,EN}$is the unavoidable exergy destruction of components in the system due to technical limitations, $\dot{E}_{D,k}^{UN,EX}$ is an unavoidable exogenous part due to the technical limitations of other parts of the system except this part, $\dot{E}_{D,k}^{AV,EN}$ can be improved by increasing the efficiency of components, which is an avoidable endogenous part, $\dot{E}_{D,K}^{AV,EX}$can be reduced by improving the efficiency of the system or other components, which is an avoidable exogenous part [15].

3.4. Simulation analysis model

Considering the source of exergy destruction in the system, it is necessary to analyze the main components of the system. The exergy destruction caused by temperature difference transmission in the heat exchanger is expressed as ΔT_{GC} and ΔT_{EVA}. There are nozzle, mixing chamber and diffuser in the ejector, and there are many kinds of exergy destruction. The exergy destruction of this part is expressed by η_n, η_m,η_m and η_d parameters. Exergy destruction in the compressor is represented by η_{LPC} and η_{HPC}.The actual cycle, ideal cycle, mixed cycle and unavoidable cycle are established according to the Table 2., and the above parameters are calculated according to the established model. Figure 2. shows the calculation flow chart of energy analysis, conventional and advanced exergy analysis. In this study, EES (Engineering equation solver) is used to write the program language of the model, and the physical parameters of the working fluid used by the standard IIR database of the international refrigeration society. Table 3 and table 4 show the thermodynamic data of working fluid when the cycle operates under actual and unavoidable conditions respectively.

Table 2. Parameters used in the real, ideal and unavoidable conditions.

Component	Parameter	Real condition	Ideal condition	Unavoidable condition
Gas cooler (GC)	ΔT_{GC}	8.00℃	0	0.50℃
Evaporator (EVA)	ΔT_{EVA}	2.00℃	0	0.50℃
HP compressor (HPC)	η_{LPC}	0.84	1	0.95
LP compressor (LPC)	η_{HPC}	0.84	1	0.95
Ejector (EJE)	η_n	0.75	$E_{D,EJE} = 0$	0.8

	η_m	0.90		0.95
	η_d	0.90		0.95
Expansion valve1 (EV1)	-	Isenthalpic	Isenthalpic	Isenthalpic
Expansion valve2 (EV2)	-	Isenthalpic	Isenthalpic	Isenthalpic

Table 3. State point parameters of system cycle under real conditions.

state	Fluid	m/(kg/s)	T/℃	P/MPa	h/(kJ/kg)	s/(kJ/(kg·K))
1	CO2	0.1607	9	4.4	423.8	1.791
2	CO2	0.1607	68	9.3	456.3	1.806
3	CO2	0.1607	35	9.3	295.1	1.302
4	CO2	0.1607	30	9.3	274.6	1.235
5	CO2	0.1928	9	4.4	325.2	1.441
6	CO2	0.0676	9	4.4	223.2	1.08
7	CO2	0.0676	-35	1.2	223.2	1.129
8	CO2	0.0676	-35	1.2	436.2	2.023
9	CO2	0.0676	14	1.2	484.9	2.21
10	CO2	0.0676	131	4.6	577.8	2.246
11	CO2	0.0351	130	4.4	577.8	2.254
12	Water	0.177	26	0.1	109.1	0.381
13	Water	0.177	61	0.1	255.4	0.844
14	Air	2.86	-25	0.1	248.1	6.675
15	Air	2.86	-30	0.1	243.1	6.655
0	Air	-	25	0.1	298.4	6.86

COP:1.252, W_{HPC} :6.281kW, W_{LPC}:5.222kW, Q_e:14.4kW, R_{mf}:0.42

Table 4. State point parameters of system cycle under unavoidable conditions.

state	Fluid	m/(kg/s)	T/℃	P/MPa	h/(kJ/kg)	s/(kJ/(kg·K))
1	CO2	0.1571	9	4.4	423.8	1.791
2	CO2	0.1571	67	9.3	452.7	1.806
3	CO2	0.1571	35	9.3	295.1	1.302
4	CO2	0.1571	30	9.3	274.6	1.235
5	CO2	0.1885	9	4.4	323.9	1.441
6	CO2	0.0675	9	4.4	223.2	1.08
7	CO2	0.0675	-33.5	1.2	223.2	1.129
8	CO2	0.0675	-33.5	1.2	436.4	2.023
9	CO2	0.0675	13.5	1.2	484.1	2.21
10	CO2	0.0675	127	4.6	570.2	2.246
11	CO2	0.0361	123	4.4	570.2	2.254
12	Water	0.169	26	0.1	109.1	0.381
13	Water	0.169	61	0.1	255.4	0.844
14	Air	2.88	-27.5	0.1	245.6	6.669
15	Air	2.88	-32.5	0.1	240.6	6.649
0	Air	-	25	0.1	298.4	6.86

COP:1.391,W_{HPC} :4.47kW, W_{LPC}:5.54kW, Q_e:14.4kW, R_{mf}:0.44

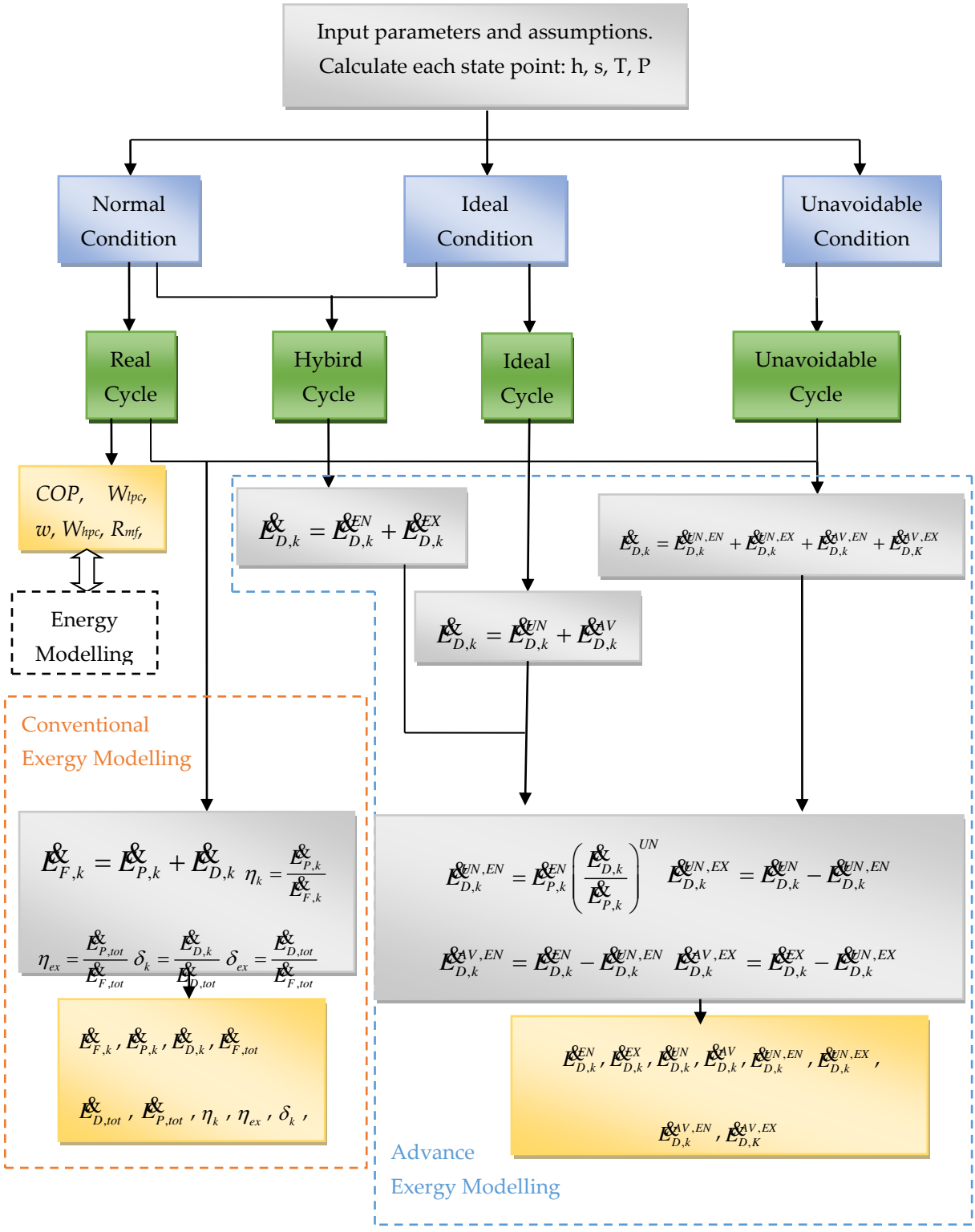

Figure 2. Flowchart of the simulation procedure with energy, conventional and advanced analyses.

3.4. Modelling validation

The model is verified by energy analysis and conventional exergy analysis. Comparing the COP of energy analysis with the data in Eskandari's article[8], it can be found from the figure 2 that the change trend of the system with the gas cooler pressure is very consistent with that of [8].

The parameters of the preset initial state points in the system are shown in Table 5. The calculation program is written by EES (Engineering equation solver). The calculation standard obtains the thermodynamic properties of the refrigerant by calling the standard IIR database of the international refrigeration society. On this basis, the model is verified with the data, and the verification results are shown in Figure 3. The trend of this model is similar to that of the reference literature.

Table 5. Parameters and assumptions of the system for base case.

Parameters	Present work	Eskandari [8]
η_n	0.75	0.8
η_s	0.9	0.9
η_m	0.9	0.9
P_e/MPa	3.96	3.96
P_{gc}/MPa	10.0	10.0
P_i/MPa	5.3	5.3
T_{gc}/℃	40	40
ΔT_r/℃	5	5

Figure 3. The assumed parameters are compared with the simulation results and Eskandari [8].

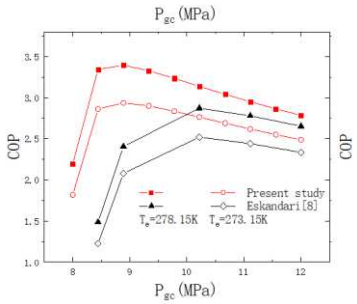

4. Results and discussion

According to the Figure 2., the energy, conventional exergy and advanced exergy of the system are simulated by EES, and its exergy performance is evaluated. Table 6 and Figure 4 list the data under the conventional exergy analysis of the system cycle and the respective proportion of exergy of each component. It can be found that the system exergy efficiency of the low-pressure compressor is the highest (η_{LPC}=88.35%), and its exergy destruction is 0.732kW, accounting for 11.91% of the total exergy destruction (δ_{LPC}=11.91%). And the part with the largest exergy destruction in the system is the ejector, which brings exergy destruction of 1.348kW to the system (δ_{EJE}= 21.93%). According to the results of conventional exergy analysis, the system should put the improvement of ejector in the first place, followed by the expansion valve 1(δ_{EV1}=15.98%), after is the evaporator (δ_{EVA}=14.28%), LP-compressor (δ_{LPC}=11.91%), high-pressure compressor (δ_{HPC}=11.61%), intercooler (δ_{ITC}=9.42%), internal heat exchanger (δ_{ITE}=6.2%), gas cooler (δ_{GC}=5.11%) and expansion valve 2 (δ_{EV2}=2.68%). At this time, the total exergy efficiency of the system is 23.94%.

Table 7. and Figure 5. display the results of advanced exergy analysis and the proportion of each component's exergy, the advanced exergy analysis gives more detailed insights of the operating characteristics with avoidable/unavoidable and endogenous/exogenous parts [30]. Figures signify that: (1) Advanced exergy analysis divides exergy destruction into endogenous and exogenous parts suggests that the system have larger $\dot{E}_{D,k}^{EN}$ than $\dot{E}_{D,k}^{EX}$ with most components in the system, which indicates that it is mainly caused by the component itself. The value of $\dot{E}_{D,EVA}^{EX}$ is exactly the same as that of $\dot{E}_{D,EVA}$, because the evaporator is used to maintain the refrigeration capacity of a fixed system, and its exergy output is fixed, which is independent of other components and completely caused by its own irreversibility [29],which is also reflected in the article [31], and besides the gas cooler, the $\dot{E}_{D,k}^{EN}$ in the system is always greater than the $\dot{E}_{D,k}^{EX}$, this shows that the gas cooler needs to be optimized through the improvement of other components; (2) Advanced exergy analysis divides exergy destruction into unavoidable and avoidable parts indicates that the system have larger $\dot{E}_{D,k}^{UN}$ than $\dot{E}_{D,k}^{AV}$ with most components in the system, while the LPC and HPC have the opposite behaviors; (3) Combining the two spitting approaches demonstrates that the system the compressor is dominated by $\dot{E}_{D,k}^{AV,EN}$ and $\dot{E}_{D,k}^{AV,EX}$, which its optimization potential is great. It can be optimized from the components themselves, but also by improving other components. The gas cooler has large proportion of $\dot{E}_{D,GC}^{UN,EN}$ and $\dot{E}_{D,GC}^{UN,EX}$, so it does not have much optimization potential. Due to

its own limitations($\dot{E}_{D,EVA}^{UN,EN}$), the exergy destruction of evaporator cannot be reduced by other methods. There is a negative value in the exergy destruction value of expansion valve and ejector in the component ($\dot{E}_{D,EV1}^{UN,EN}$, $\dot{E}_{D,EJE}^{UN,EN}$), that is, other components have a positive effect on the component, and this part will increase when the efficiency of other remaining components is improved. Focus on $\dot{E}_{D,k}^{AV,EN}$ and $\dot{E}_{D,k}^{AV,EX}$ (Column 9 and 10 of Table 7.), which represents the improvement that can be achieved by the component itself and the improvement impact of other components on the component, and can be used to guide system enhancement [31]. Among them, $\dot{E}_{D,k}^{AV,EN}$is the factor to improve its own components, and the mutual factors between components are too complex. Generally, only this factor is considered when considering the improvement of system performance. The optimization of components is sorted according to the value, and the results are as follows: ejector (34.35%), HP-compressor (31.37%), LP-compressor (14.5%), evaporator (8.53%), expansion valve 2 (5.98%), intercooler (2.53%),expansion valve 1 (2.0%), gas cooler (0.51%), internal heat exchanger (0.23%). It can be seen that the optimization potential of ejector is second only to compressor.

According to the results of conventional and advanced exergy analysis in Table 8, there are obvious differences in the optimization sequence of system components. The difference between the two is that conventional exergy methods focus on the total exergy destruction of components, while advanced exergy analysis considers components themselves, the relationship between other components in the system, and economic and technical limitations [32].

Table 6. Results of conventional exergy analysis.

Equipment	$\dot{E}_{F,k}$ (kW)	$\dot{E}_{P,k}$ (kW)	$\dot{E}_{D,k}$ (kW)	$\dot{E}_L$ (kW)	η_k/%	δ_k/%
LPC	6.281	5.549	0.7321	-	88.35	11.91
HPC	5.222	4.509	0.7136	-	86.35	11.61
GC	1.775	1.461	0.3139	-	82.31	5.11
EJE 1	1.757	0.4089	1.348	-	23.27	21.93
EV 1	5.09	4.108	0.9824	-	80.71	15.98
EV 2	0.7637	0.5991	0.1647	-	78.45	2.68
ITC	0.8945	0.3155	0.579	-	35.27	9.42
ITE	0.4628	0.08167	0.3811	-	17.65	6.20
EVA	3.632	2.754	0.8781	-	75.83	14.28
TES	-	-	-	-	-	-
Total	11.503	2.754	6.0929	2.6561	23.94	100
δ_{ex}			52.97%			

Table 7. Results of advanced exergy analysis.

Component	$\dot{E}_{D,k}$	Splitting the exergy destruction				Combined two splitting approaches			
		$\dot{E}_{D,k}^{EN}$	$\dot{E}_{D,k}^{EX}$	$\dot{E}_{D,k}^{AV}$	$\dot{E}_{D,k}^{UN}$	$\dot{E}_{D,k}^{UN,EN}$	$\dot{E}_{D,k}^{UN,EX}$	$\dot{E}_{D,k}^{AV,EN}$	$\dot{E}_{D,k}^{AV,EX}$
LPC	0.7321	0.6846	0.0475	0.2039	0.5282	0.4856	0.0426	0.1990	0.0049
HPC	0.7136	0.6017	0.1119	0.5105	0.2031	0.1713	0.0319	0.4304	0.0800
GC	0.3139	0.3079	0.006	0.011	0.3029	0.3008	0.0021	0.0071	0.0039
EJE 1	1.3488	1.161	0.1878	0.477	0.8718	0.6897	0.1820	0.4713	0.0058
EV 1	0.9824	0.9432	0.0392	0.0604	0.922	0.9157	0.0063	0.0275	0.0329
EV 2	0.1647	0.1861	-0.021	0.0005	0.1642	0.1041	0.0601	0.0820	-0.082
ITC	0.579	0.408	0.171	0.109	0.47	0.3733	0.0967	0.0347	0.0743
ITE	0.3811	0.0896	0.2915	0.0061	0.3749	0.0864	0.2885	0.0032	0.0030
EVA	0.8781	0.8781	0	0.1171	0.761	0.7610	0.0000	0.1171	0
Total	6.0937	5.2602	0.8335	1.4955	4.5982	3.888	0.7102	1.3722	0.1233

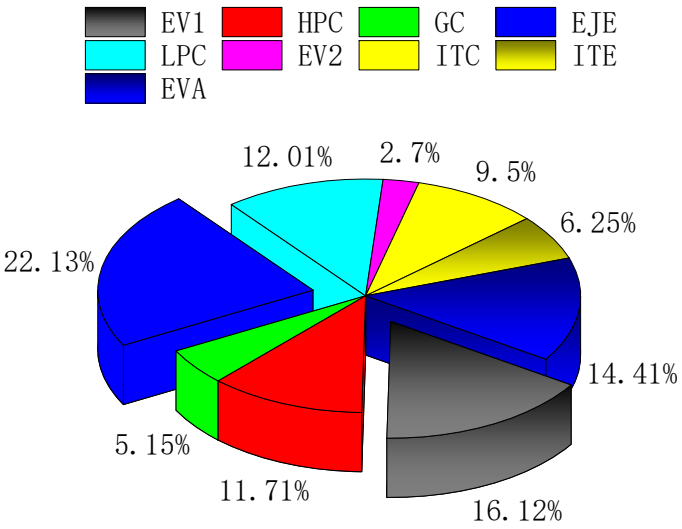

Figure 4. Proportion diagram of exergy destruction of each component.

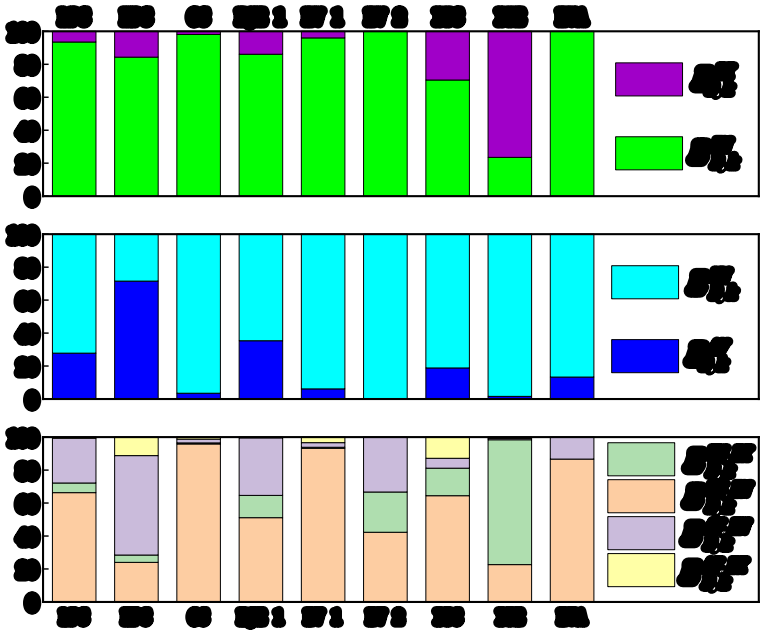

Figure 5. Advance exergy analysis of exergy destruction of each component.

Table 8. Improvement priority of component based on conventional and advanced exergy analyses.

Precedence	Conventional exergy analysis ($\dot{E}_{D,k}$)	Advance exergy analysis ($\dot{E}_{D,k}^{AV,EN}$)
1	Ejector	Ejector
2	Expansion valve 1	HP-compressor

3	Evaporator	LP-compressor
4	LP-compressor	Evaporator
5	HP-compressor	Expansion valve 2
6	Intercooler	Intercooler
7	Internal heat exchanger	Expansion valve 1
8	Gas cooler	Gas cooler
9	Expansion valve 2	Internal heat exchanger

5. Results and discussion

In order to observe the exergy destruction characteristics of various components and evaluate the performance of the system, it is very important to observe the changes of the system under different working conditions. In this section, the key parameters of P_e, T_{gc} and P_{gc} of heat exchangers are changed as input, and P_i, a very important parameter in two-stage compression, is also adjusted as input. In addition, COP is an important parameter that can be intuitively expressed in energy analysis. η_{ex} and $E_{D,tot}$ represent the overall exergy characteristics of the system, $E_{D,k}$ represents the conventional exergy level, $\dot{E}_{D,k}^{EN}$ and $\dot{E}_{D,k}^{EX}$ are represent the endogenous or exogenous exergy destruction of a system component, $\dot{E}_{D,k}^{AV}$ is the avoidable of the total avoidable exergy destruction of the component, while $\dot{E}_{D,k}^{AV,EN}$ is the endogenous exergy destruction of the component, which is an important parameter in advanced exergy. Therefore, the above four parameters represent the level of advanced exergy. Finally, while discussing one variable, the parameters of other variables are fixed and set to the corresponding conditions under actual conditions (column 3 of Table 5.).CO_2 is used as refrigerant in this system, The operating conditions are locally adjusted according to the basic working conditions in Table 2: the evaporation pressure (P_e) of the evaporator is in the range of 1.2MPa ~ 2.0MPa; the working pressure range of intermediate pressure(P_i) is 2.0-5.0MPa; the outlet temperature (T_{gc}) and pressure of the gas cooler (P_{gc}) in the range of 30 ~ 40 ℃ and 9.0 ~ 12.0MPa; the refrigerant at the outlet of the evaporator is saturated; after the refrigerant from the gas cooler flows through the internal heat exchanger, the superheat is 5℃, and the enthalpy of the refrigerant flowing from the evaporator into the internal heat exchanger is calculated from the relationship between energy and mass. According to the above working conditions, the effects of P_{gc}, T_{gc}, P_i and P_e on system performance and performance are analyzed.

5.1. Effect of gas cooler pressure on system energy and exergy analysis results

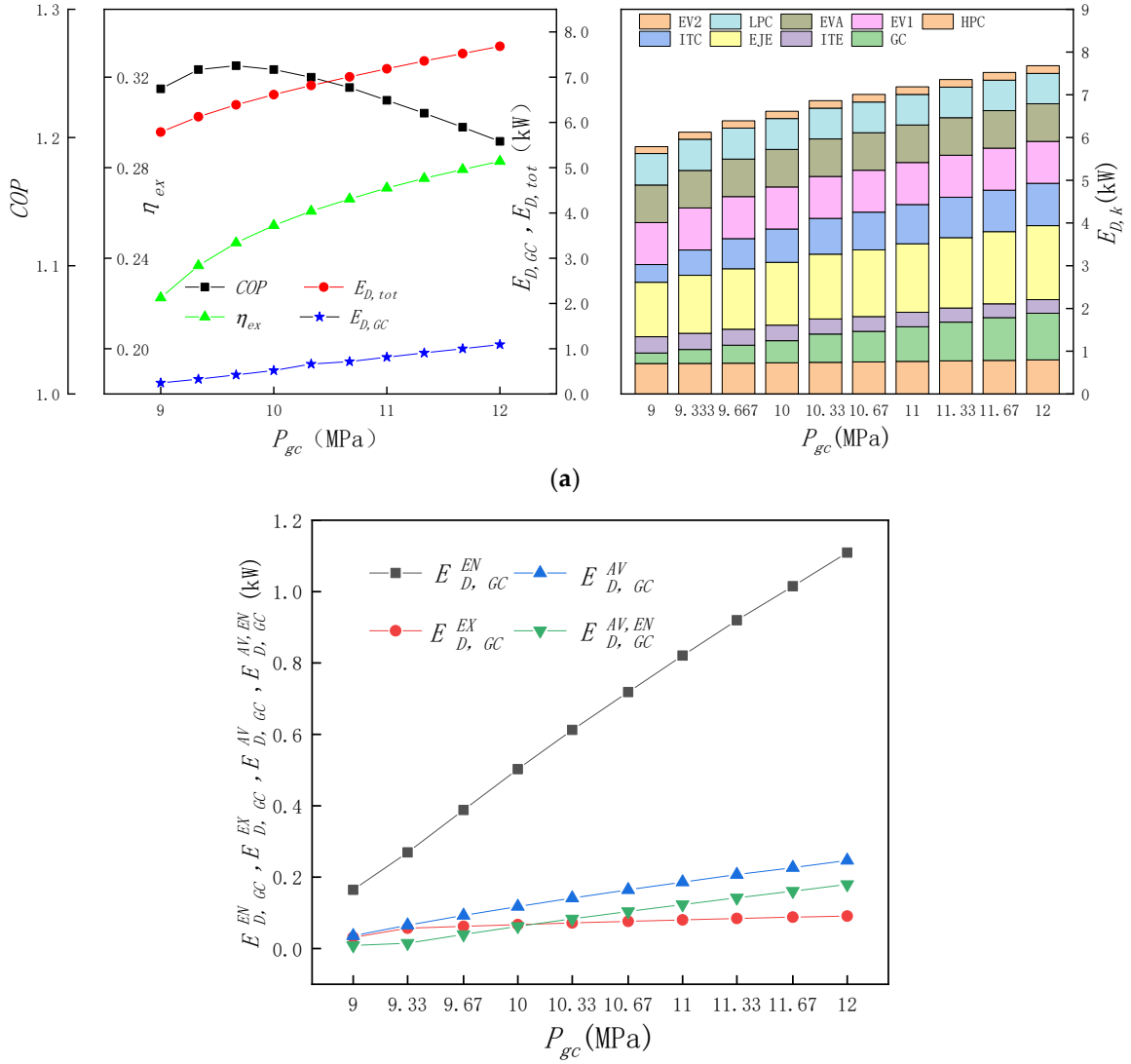

Figure 6. (a) Influence of system energy and conventional exergy with P_{gc}. **(b)**. Effect of the P_{gc} difference in the gas cooler with advanced exergy

The P_{gc} has a great influence on the performance of a two-stage compression refrigeration system with transcritical CO_2. Therefore, from the energy and conventional exergy analysis of Figure 6(a), the COP, total exergy destruction and exergy efficiency of the system change with P_{gc}. This figure shows the changes of system performance and exergy performance, including the middle pressure and evaporation pressure of the system. And gas cooler outlet temperature remains unchanged (P_i=4.4MPa, P_e=1.2MPa, T_{gc}=35℃). It can be found that there is a P_{gc} of 9.75 MPa. Under this P_{gc}, the system has a maximum COP of 1.256 under this range. From the exergy efficiency curve, it can be seen that the rise rate of exergy efficiency is the lowest at this pressure, and after that, keep the rate rising steadily. The total exergy destruction of the system and the exergy destruction of gas cooler components increase with the change of gas cooler pressure. From the cumulative change of exergy destruction of system components when P_{gc} changes, with the increase of P_{gc}, no matter the increase or decrease of exergy destruction of other components of the system, the exergy destruction of gas cooler components will increase. And it can be observed that the exergy destruction of ejector components increases, which is due to the increase of P_{gc} and the increase of various states of working medium at the mainstream inlet of ejector, resulting in the increase of exergy destruction of this component, and the exergy destruction of other components remains basically

stable. From the advanced exergy analysis of Figure 6(b), it can be seen that the endogenous exergy destruction of components increases rapidly compared with the exogenous exergy destruction ($\dot{E}_{D,GC}^{EN}$ and $\dot{E}_{D,GC}^{EX}$ increase by 0.2kW and 0.06kW respectively for every 1MPa increase of P_{gc}). At 12MPa, $\dot{E}_{D,GC}^{EN}$ accounts for 92.4% of the exergy destruction of the whole components' exergy destruction, and accounts for a larger proportion in the exergy destruction of components with the increase of P_{gc}. Exogenous exergy destruction was basically maintained at a low level. This is because the pressure rise of the gas cooler directly affects the parameters of the inlet and outlet of the gas cooler, which has little impact with other parts. Both $\dot{E}_{D,GC}^{AV}$ and $\dot{E}_{D,GC}^{AV,EN}$ increase with the increase of P_{gc}, but the increase is relatively slow (0.1066kW and 0.055kW per 1MPa respectively), and they account for less of the overall exergy destruction, which means that the optimization degree of this part is low.

5.2. Energy and exergy analysis results of the system at gas cooler outlet temperature

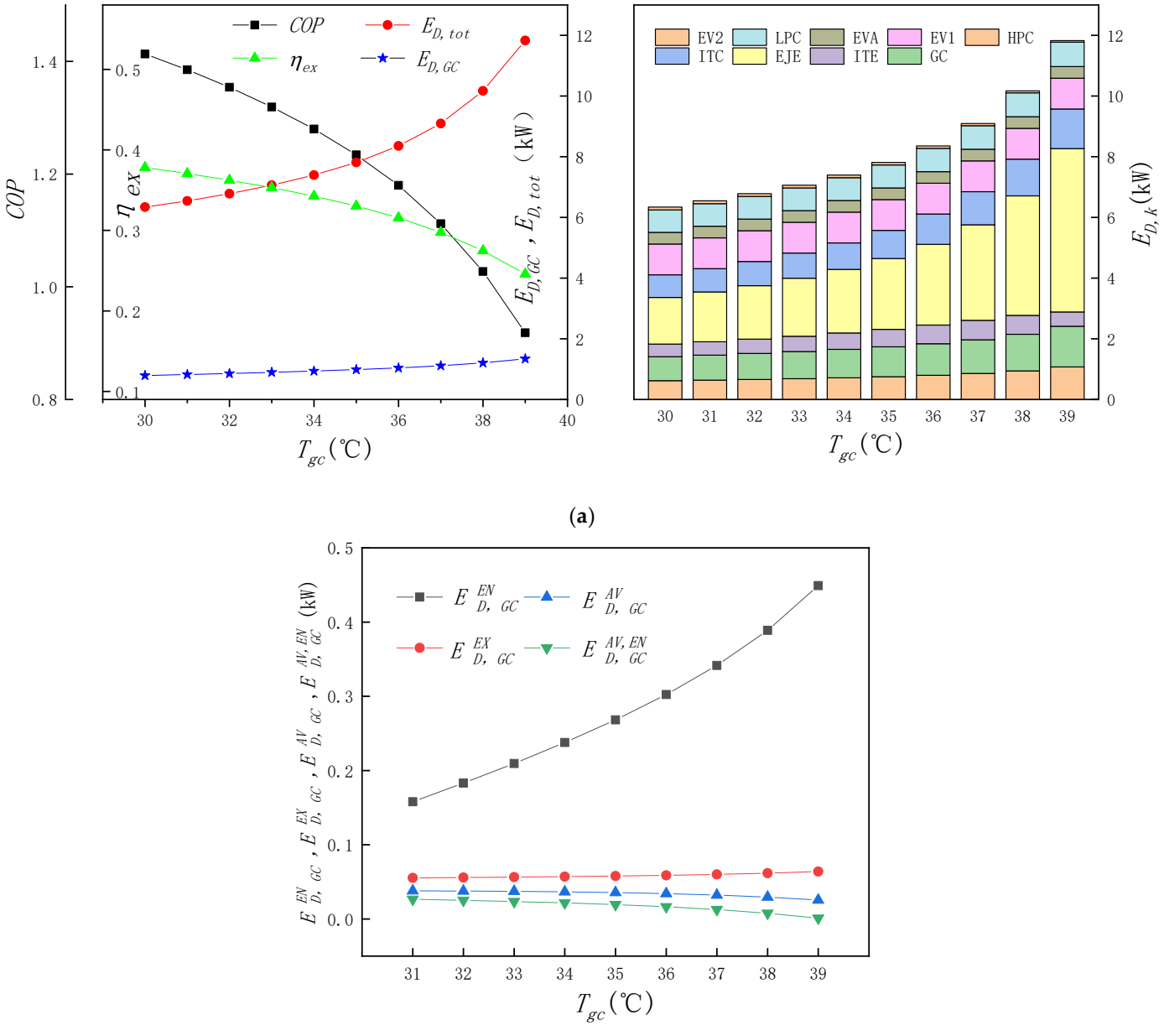

Figure 7. (a). Influence of system energy and conventional exergy with T_{gc}. **(b)**. Effect of the T_{gc} difference in the gas

cooler with advanced exergy.

The T_{gc} is directly related to the cooling effect of the gas cooler, directly reflects the cooling capacity of the gas cooler components, and has a great impact on the front and rear components of the gas cooler, especially on the ejector components. Therefore, this section discusses the influence of the T_{gc} 30-39℃ on the system performance and exergy performance of Figure 7(a). The P_e, P_i and P_{gc} remain unchanged (P_i = 4.4MPa, P_e = 1.2MPa, P_{gc} = 9.3MPa). The figure shows that with the increase of the T_{gc}, the COP of the system is obviously in a downward trend. This is because the increase of the T_{gc} means that the cooling capacity of the gas cooler decreases, and the high-temperature and high-pressure refrigerant cannot be cooled, resulting in higher working conditions of the following components, and the $E_{D,tot}$ of the system also increases straight up. The figure shows the accumulation change diagram of each component exergy destruction of the system with the change of T_{gc} at 30-39℃. It can be observed from the figure that with the increase of the T_{gc}, the total exergy destruction of the system always increases gradually. At the same time, the $E_{D,EJE}$ increases sharply, and the proportion in the $E_{D,tot}$ also increases. This is because with the increase of the T_{gc}, the state parameters of the main flow inlet refrigerant of the ejector are at a high state point. At the same time, according to the equation (9), with the increase of its enthalpy, the enthalpy of the refrigerant injected from the ejector also increases, that is, the gaseous state of the refrigerant in the two-phase flow increases, the liquid state decreases, and the refrigerant to the low-pressure stage also decreases. To achieve the preset refrigeration effect, it is necessary to improve the overall mass flow to ensure the refrigeration effect of the evaporator, and the overall exergy destruction of the system also increases. From the advanced exergy analysis of Figure 7(b), the $E_{D,GC}$ also increases with the increase of T_{gc}, and most of the increase comes from the $\dot{E}_{D,GC}^{EN}$, and the $\dot{E}_{D,GC}^{EX}$ remains basically unchanged with the increase of T_{gc}, because the outlet temperature of gas cooler directly affects the system components, T_{gc} becomes the main variable, causing changes in other components. Therefore, it can be seen from the figure that only the $\dot{E}_{D,GC}^{EN}$ increases with the increase of T_{gc}, and $\dot{E}_{D,k}^{AV}$ and $\dot{E}_{D,GC}^{AV,EN}$ in components tend to decrease with the increase of T_{gc}, but the overall exergy destruction is small and the optimization potential is low.

5.3. Analysis results of influence of evaporator pressure on system energy and exergy

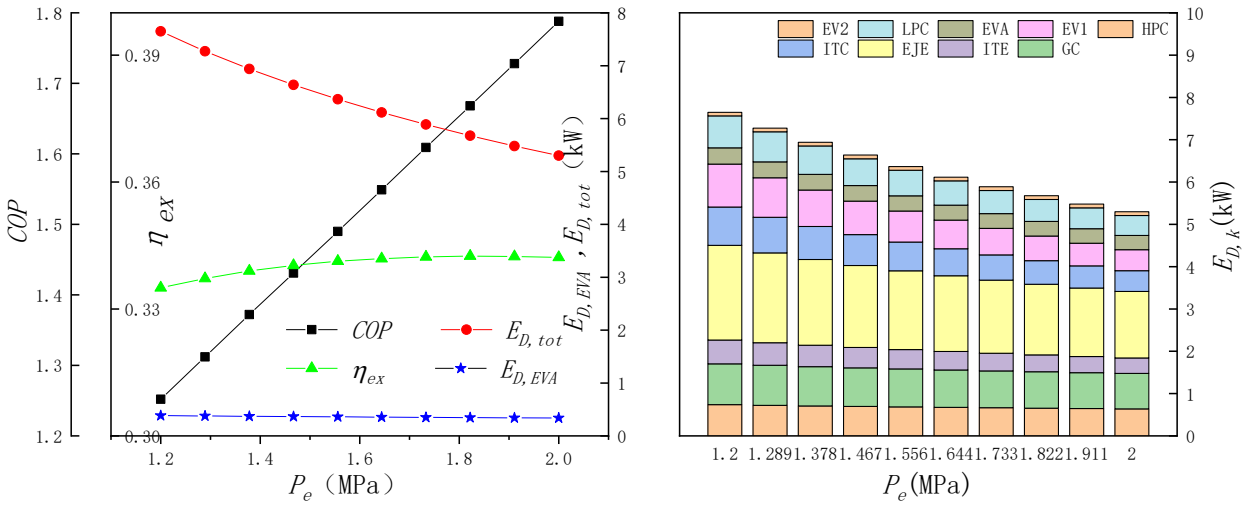

(**a**)

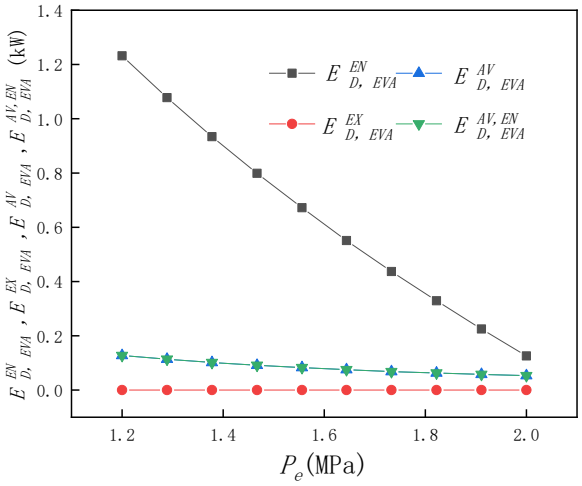

(b)

Figure 8. (a). Influence of system energy and conventional exergy with P_e. **(b).** Effect of the P_e difference in the evaporator with advanced exergy

The P_e represents the lowest temperature that the refrigeration system can reach. Changing P_e changes all components in the low-pressure area of the system and can have a significant impact on the system. This section discusses the influence of P_e on system performance and exergy performance under the pressure of 1.2-2.0 MPa and exergy destruction of various parts of evaporator components, in which the P_i, P_{gc} and T_{gc} of the system remain unchanged (P_i = 4.4MPa, P_{gc} = 9.3MPa, T_{gc} = 35 ℃). The Figure 8(a) shows that with the increase of P_e, the COP of the system increases linearly, which is common in all refrigeration systems; The total exergy destruction of the system is reduced because the overall increase of the pressure in the low-pressure area of the system leads to the reduction of the exergy destruction of all working parts, and it can be predicted that the change of P_e has little impact on all parts in the high-pressure area. This figure shows the cumulative exergy destruction of each component of the system with the change of P_e. With the increase of P_e, ejector components still account for the main part of the total exergy destruction of the system. The exergy destruction of ejector components decreases gradually, but the proportion of total exergy destruction of the system increases slightly. This is because with the increase of P_e, the mass flow of the low-pressure stage increases slightly, and the mass flow of the ejector increases slightly to achieve the predesigned refrigeration load. From the exergy destruction of the evaporator, it can be found that the change value is not obvious, because the rise of P_e only affects the enthalpy value of the evaporator outlet (the evaporator outlet is saturated), and the exergy destruction of components is slightly reduced. However, this change can be seen more clearly from the advanced exergy of Figure 8(b). With the increase of P_e, $\dot{E}^{EX}_{D,EVA}$ is always 0, and the change of component exergy destruction is completely represented by $\dot{E}^{EN}_{D,EVA}$, which indicates that the exergy of evaporator is completely endogenous. Therefore, there is no difference between $\dot{E}^{AV}_{D,EVA}$ and $\dot{E}^{AV,EN}_{D,EVA}$, that is, the two curves coincide completely.

5.4. Analysis results of the effect of intermediate pressure on the energy and exergy of the system

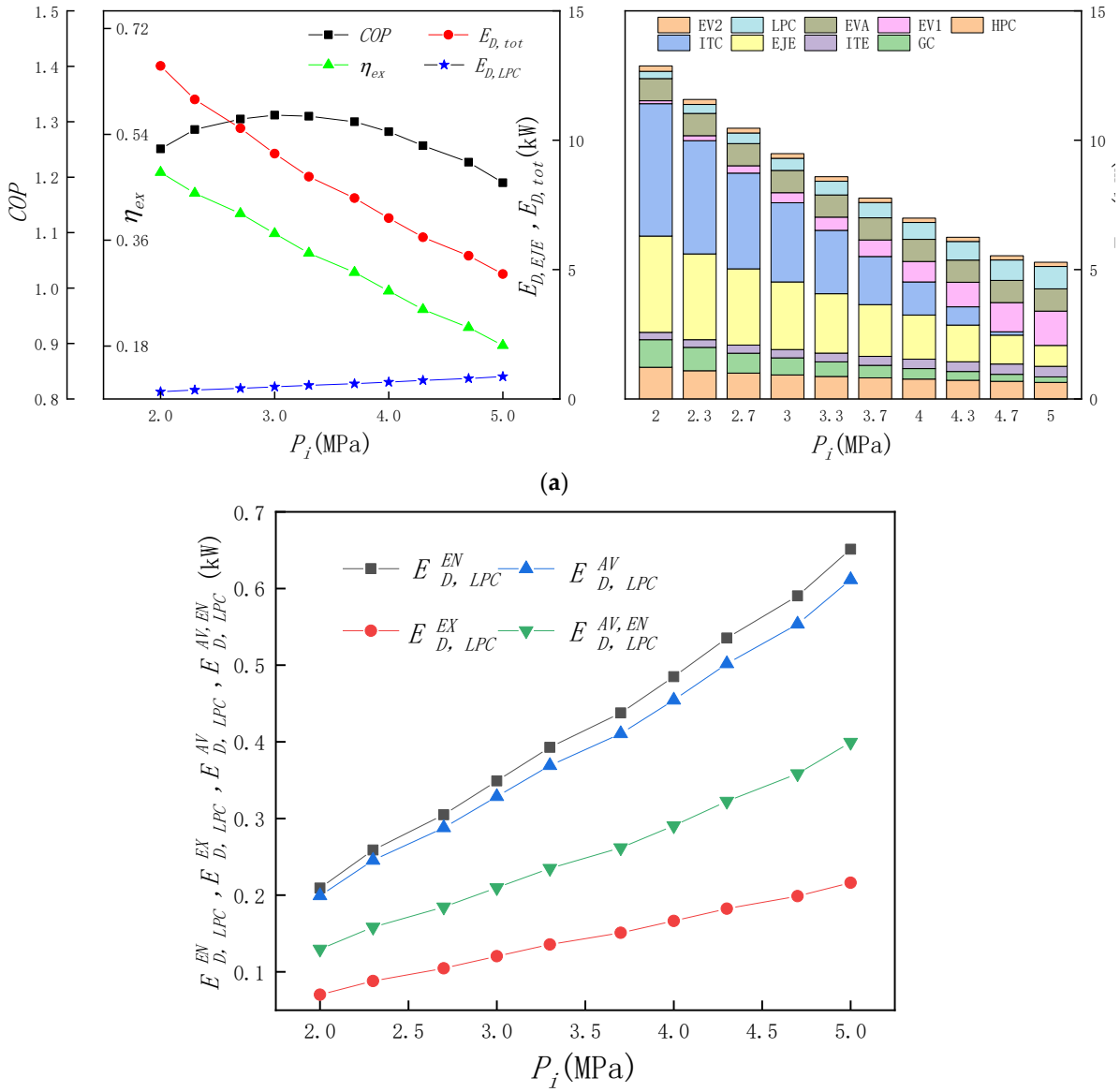

Figure 9. (a). Influence of system energy and conventional exergy with P_i. **(b).** Effect of the P_i difference in the LP-compressor with advanced exergy.

Intermediate pressure is the characteristic of two-stage compression refrigeration system. There is always an optimal P_i value in two-stage compression to maximize system performance and affect the inlet–outlet pressure ratio of low-pressure and high-pressure compressors. Therefore, P_i value is a key parameter affecting system performance. This section discusses the impact of P_i on system performance and exergy performance under the change of 3.0-5.0MPa in Figure 9(a), including the impact of keeping the P_{gc}, P_e and T_{gc} of the system unchanged (P_{gc} = 9.3MPa, P_e = 1.2MPa, T_{gc} = 35℃) on system performance and exergy performance and each exergy destruction of LPC under advanced exergy analysis. This figure shows the system performance as P_i increases. It can be found that with the increase of P_i, the total exergy destruction of the system decreases linearly. Under this pressure, when the P_i of the system is 3.0MPa, the COP of the system reaches the maximum value of 1.316. This figure shows that when the system pressure changes at the intermediate pressure, this pressure is the peak of the system performance under two-stage compression. The figure shows the cumulative exergy destruction of each component. It can be seen from the figure that with the increase of P_i, the total exergy destruction of the system decreases linearly, and the exergy destruction of the intercooler in the system decreases rapidly after occupying the main part of the to-

tal exergy destruction. The intercooler is mainly due to the high enthalpy at the outlet of the intercooler due to the low P_i, and the low enthalpy of the refrigerant from the low-pressure compressor and ejector. The exergy destruction of ejector components decreases because P_i is directly related to the outlet pressure of ejector. With the increase of P_i, the state of refrigerant from low-pressure compressor increases, resulting in the decrease of exergy enthalpy. It can also be seen from the performance of exergy destruction of LPC in advanced exergy analysis of Figure 9(b) that $\dot{E}_{D,LPC}^{EN}$, $\dot{E}_{D,LPC}^{EX}$,$\dot{E}_{D,LPC}^{AV}$ and $\dot{E}_{D,LPC}^{AV,EN}$ all maintain an upward trend, Its $\dot{E}_{D,LPC}^{AV}$ always accounts for a high proportion with the increase of P_i, which shows that the low-pressure compressor has a certain optimization potential. In addition, the increase of P_i also changes the flow ratio of high and low pressure section, resulting in the exergy destruction of gas cooler and other components, maintaining a stable downward trend.

6. Conclusions

In the work of this paper, the energy, conventional exergy system model and advanced exergy system model of supercritical CO_2 refrigeration system with ejector are established, the cycle performance and two kinds of exergy failure of the system are calculated, and the exergy failure characteristics of various components in the system are analyzed and compared. At the same time, through two analysis methods, the improvement potential and order of system components are determined respectively. Finally, the main parameters in the system are analyzed to determine the impact of the main parameters on the system performance and the exergy performance of each component. It is observed that the main parameters have a great impact on those components. The main research results of this paper are summarized as follows:

(1) According to the established energy and two exergy analysis models, the system has great optimization and improvement potential. According to the operating parameters of the system model established in this paper under the basic conditions and the results of conventional exergy analysis, the main optimization objects of the system are ejector, expansion valve 1 and evaporator, accounting for 22.13%, 16.12% and 14.41% of the total exergy destruction respectively. At this time, the exergy efficiency of the system is 23.94% and the COP of the system is 1.252. According to the analysis of advanced exergy, the improvement of system components should focus on ejector and high and low pressure compressor.

(2) The results of advanced exergy analysis model show that the endogenous exergy of each component in the system is always greater than the exogenous exergy, and the overall endogenous exergy destruction accounts for 86.32% of the total exergy destruction, which indicates that the exergy destruction of the system is mainly related to the component itself, and the interdependence with other components is low. In addition, after calculation, it is found that in the advanced exergy analysis, the ejector and high-pressure ejector account for the main part of the exergy destruction that can be avoided (66.03%).

(3) According to the established energy and two exergy analysis models, the main parameters in the system cycle are changed in a certain range to observe the influence of these parameters on the system performance and the exergy performance of various components of the system. Among them, the two parameters of gas cooler pressure and intermediate pressure have a great impact on the system. Both of them have an optimal value, which can maximize the performance of the system.

(4) It is considered that the exergy destruction of the compressor is the highest in the exergy optimization system, and the exergy destruction can be avoided in the exergy optimization of the compressor.

Abbreviations

Symbols		*Subscripts*	
CO_2	Carbon dioxide	*o*	Out of ejector
ex	Specific exergy (kJ kg^{-1})	*D*	Exergy destructions
E	Exergy flow rate (kW)	*h*	High pressure side fluid
EES	Engineering equation solver	*l*	Low pressure side fluid
h	Specific enthalpy (kJ kg-1)	*mf*	Refrigerant mass flow
m	Mass flow rate (kg s^{-1})	*d*	diffuser
P	Pressure (MPa)	*r*	Superheat
W	Compressor work (kW)	*ex*	Exergy
Q	Refrigerating capacity (kW)	*i*	Intermediate
s	Entropy (kJ kg^{-1} K^{-1})	*F*	Fuel
T	Temperature (K)	*P*	Production
ΔT	Temperature difference (K)	*j*	exergy carrier positions
LPC	Low pressure compressor	*const*	Constant
HPC	High pressure compressor	*UN*	Unavoidable
GC	Gas cooler	*AV*	Avoidable
EVA	Evaporator	*L*	loss
EJE	Ejector	*EN*	Endogenous
*EV*1	Low pressure expansion valve	*EX*	Exogenous
*EV*2	Medium pressure expansion valve	*k*	kth component
ITC	Intercooler	*m*	Mixing chamber
ITE	Internal heat exchanger	*n*	Nozzle
		s	Suction chamber
Greek symbols		*is*	Isentropic
		tot	Total
η	Efficiency	0	Reference condition
w	Entrainment ratio	1–11	Location
δ	Rate of exergy destruction	*Gen*	Entropy production

References

1. Zhang, Q.; Luo, Z. Thermodynamic analysis and multi-objective optimization of a transcritical CO2 waste heat recovery system for cruise ship application. *Energy Convers. Manage*, **227**, 113612.https://doi.org/10.1016/j.enconman.2020.113612 (2021).
2. Artuso, P.; Rossetti, A. Dynamic modeling and thermal performance analysis of a refrigerated truck body during operation. *Int. J. Refrig.*, **99**, 288-299.https://doi.org/10.1016/j.ijrefrig.2018.12.014 (2019).
3. Yu, A.; Su, W. Thermodynamic analysis on the combination of supercritical carbon dioxide power cycle and transcritical carbon dioxide refrigeration cycle for the waste heat recovery of shipboard. *Energy Convers. Manage*, **221**, 113214.https://doi.org/10.1016/j.enconman.2020.113214 (2020).
4. Liang, Y.; Sun, Z. Investigation of a refrigeration system based on combined supercritical CO2 power and transcritical CO2 refrigeration cycles by waste heat recovery of engine. *Int. J. Refrig.*, **118**, 470-482.https://doi.org/10.1016/j.ijrefrig.2020.04.031 (2020).
5. Yu, B.; Yang, J. An updated review of recent advances on modified technologies in transcritical CO2 refrigeration cycle. *Energy*, **189**, 116147.https://doi.org/10.1016/j.energy.2019.116147 (2019).
6. Gullo, P.; Hafner, A. Transcritical R744 refrigeration systems for supermarket applications: Current status and future perspectives. *Int. J. Refrig.*, **93**, 269-310.https://doi.org/10.1016/j.ijrefrig.2018.07.001 (2018).
7. Kimura de Carvalho, B. Y.; Melo, C. An experimental study on the use of variable capacity two-stage compressors in transcritical carbon dioxide light commercial refrigerating systems. *Int. J. Refrig.*, **106**, 604-615.https://doi.org/10.1016/j.ijrefrig.2019.03.026 (2019).
8. Eskandari Manjili, F.; Cheraghi, M. Performance of a new two-stage transcritical CO2 refrigeration cycle with two ejectors. *Appl. Therm. Eng.*, **156**, 402-409.https://doi.org/10.1016/j.applthermaleng.2019.03.083 (2019).
9. Song, Y.; Ma, Y. Review on the simulation models of the two-phase-ejector used in the transcritical carbon dioxide systems. *Int. J. Refrig.*, **119**, 434-447.https://doi.org/10.1016/j.ijrefrig.2020.04.029 (2020).
10. Santini, F.; Di Battista, D. In *Transcritical CO2 refrigeration plants: Experimental campaign and model-based evaluations of new technologies*, AIP Conf. Proc., 2019; AIP Publishing LLC: p 020136.
11. Yang, D.; Li, Y. Research and application progress of transcritical CO2 refrigeration cycle system: a review. *Int. J. Low-Carbon Technol*.10.1093/ijlct/ctab086 (2021).
12. Nebot-Andrés, L.; Sánchez, D. Experimental determination of the optimum intermediate and gas-cooler pressures of a commercial transcritical CO2 refrigeration plant with parallel compression. *Appl. Therm. Eng.*, **189**, 116671.https://doi.org/10.1016/j.applthermaleng.2021.116671 (2021).
13. Liu, Y.; Liu, J. Theoretical analysis on a novel two-stage compression transcritical CO2 dual-evaporator refrigeration cycle with an ejector. *Int. J. Refrig.*, **119**, 268-275.https://doi.org/10.1016/j.ijrefrig.2020.08.002 (2020).
14. Sun, Y. Y.; Wang, J. F. Performance Optimizations of the Transcritical CO2 Two-Stage Compression Refrigeration System and Influences of the Auxiliary Gas Cooler. *Energies*, **14**.10.3390/en14175578 (2021).
15. Liu, X.; Yu, K. Conventional and advanced exergy analyses of transcritical CO2 ejector refrigeration system equipped with thermoelectric subcooler. *Energy Rep.*, **7**, 1765-1779.https://doi.org/10.1016/j.egyr.2021.03.023 (2021).
16. Dahmani, A.; Aidoun, Z. Optimum design of ejector refrigeration systems with environmentally benign fluids. *Int. J. Therm. Sci.*, **50**, 1562-1572.https://doi.org/10.1016/j.ijthermalsci.2011.02.021 (2011).
17. Elbarghthi, A. F. A.; Hafner, A. An experimental study of an ejector-boosted transcritical R744 refrigeration system including an exergy analysis. *Energy Convers. Manage*, **238**.10.1016/j.enconman.2021.114102 (2021).
18. Chen, G.; Volovyk, O. Theoretical analysis and optimization of a hybrid CO2 transcritical mechanical compression – ejector cooling cycle. *Int. J. Refrig.*, **74**, 86-94.https://doi.org/10.1016/j.ijrefrig.2016.10.002 (2017).

19. Wang, X.; Yu, J. Comparative studies of ejector-expansion vapor compression refrigeration cycles for applications in domestic refrigerator-freezers. *Energy*, **70**, 635-642.https://doi.org/10.1016/j.energy.2014.04.076 (2014).
20. Ahamed, J. U.; Saidur, R. A review on exergy analysis of vapor compression refrigeration system. *Renewable Sustainable Energy Rev.*, **15**, 1593-1600.https://doi.org/10.1016/j.rser.2010.11.039 (2011).
21. Chen, J.; Havtun, H. Conventional and advanced exergy analysis of an ejector refrigeration system. *Appl. Energ*, **144**, 139-151.https://doi.org/10.1016/j.apenergy.2015.01.139 (2015).
22. Lixing, Z.; Yangdi, H. Advanced exergy analysis of a CO2 two-phase ejector. *Appl. Therm. Eng.*, 118247.https://doi.org/10.1016/j.applthermaleng.2022.118247 (2022).
23. Fallah, M.; Mohammadi, Z. Advanced exergy analysis of the combined S–CO2/ORC system. *Energy*, **241**, 122870.https://doi.org/10.1016/j.energy.2021.122870 (2022).
24. Liu, J.; Liu, Y. Performance analysis of a modified dual-ejector and dual-evaporator transcritical CO2 refrigeration cycle for supermarket application. *Int. J. Refrig.*.https://doi.org/10.1016/j.ijrefrig.2021.06.010 (2021).
25. Guang, L.; Zheyu, L. Advanced exergy analysis of ash agglomerating fluidized bed gasification. *Energy Convers. Manage*, **199**, 111952.https://doi.org/10.1016/j.enconman.2019.111952 (2019).
26. Zhan, L.; Zihui, L. Advanced exergy and exergoeconomic analysis of a novel liquid carbon dioxide energy storage system. *Energy Convers. Manage*, **205**, 112391.https://doi.org/10.1016/j.enconman.2019.112391 (2020).
27. Zhixing, J.; Jiang, Q. Advanced exergy and graphical exergy analyses for solid oxide fuel cell turbine-less jet engines. *J. Power Sources*, **456**, 227979.https://doi.org/10.1016/j.jpowsour.2020.227979 (2020).
28. Mengting, S.; Yu, Z. Advanced exergy analysis for the solid oxide fuel cell system combined with a kinetic-based modeling pre-reformer. *Energy Convers. Manage*, **245**, 114560.https://doi.org/10.1016/j.enconman.2021.114560 (2021).
29. Chen, J.; Zhu, K. Evaluation of the ejector refrigeration system with environmentally friendly working fluids from energy, conventional exergy and advanced exergy perspectives. *Energy Convers. Manage*, **148**, 1208-1224.https://doi.org/10.1016/j.enconman.2017.06.051 (2017).
30. Ozgur, B.; Hakan, A. Enhanced dynamic exergy analysis of a micro-jet (μ-jet) engine at various modes. *Energy*, **239**, 121911.https://doi.org/10.1016/j.energy.2021.121911 (2022).
31. Bai, T.; Yu, J. Advanced exergy analyses of an ejector expansion transcritical CO2 refrigeration system. *Energy Convers. Manage*, **126**, 850-861(2016).
32. Hasan, C.; Hakan, C. Advanced exergy analyses and optimization of a cogeneration system for ceramic industry by considering endogenous, exogenous, avoidable and unavoidable exergies under different environmental conditions. *Renewable Sustainable Energy Rev.* **140**, 110730.https://doi.org/10.1016/j.rser.2021.110730 (2021).

Acknowledgments

This research was funded by Shanghai Professional Technology Service Platform on Cold Chain Equipment Performance and Energy Saving Testing Evaluation (20DZ2292200).

Author Contributions

D.Z.Y. and Z.J. conceived the idea and designed the study. Z.J. and Y.L. calculate the calculation process. All authors contributed to manuscript refinement and preparation.

Competing interests

The authors declare no competing interests.

Additional information

Correspondence and requests for materials should be addressed to J.X.

Supplementary Files

This is a list of supplementary files associated with this preprint. Click to download.

- dataprocessing.xlsx